Computers and Mathematics with Applications 74 (2017) 2784–2791

Contents lists available at ScienceDirect

Computers and Mathematics with Applications

journal homepage: www.elsevier.com/locate/camwa

Nonlinear integral equations for Bernoulli's free boundary value problem in three dimensions

Olha Ivanyshyn Yaman [a], Rainer Kress [b,*]

[a] Department of Mathematics, Izmir Institute of Technology, 35430 Urla, Izmir, Turkey
[b] Institut für Numerische und Angewandte Mathematik, Universität Göttingen, 37083 Göttingen, Germany

ARTICLE INFO

Article history:
Available online 8 July 2017

Dedicated to Peter Monk on the occasion of his 60th birthday

Keywords:
Free boundary
Laplace equation
Boundary integral equation

ABSTRACT

In this paper we present a numerical solution method for the Bernoulli free boundary value problem for the Laplace equation in three dimensions. We extend a nonlinear integral equation approach for the free boundary reconstruction (Kress, 2016) from the two-dimensional to the three-dimensional case. The idea of the method consists in reformulating Bernoulli's problem as a system of boundary integral equations which are nonlinear with respect to the unknown shape of the free boundary and linear with respect to the boundary values. The system is linearized simultaneously with respect to both unknowns, i.e., it is solved by Newton iterations. In each iteration step the linearized system is solved numerically by a spectrally accurate method. After expressing the Fréchet derivatives as a linear combination of single- and double-layer potentials we obtain a local convergence result on the Newton iterations and illustrate the feasibility of the method by numerical examples.

1. Introduction

The Bernoulli problem arises in various applications such as optimal insulation, fluid dynamics, electrostatics, electro chemistry and many others, see [1] and the references therein. Mathematically the problem is formulated as follows. Let D_0 and D_1 be bounded domains in $\mathbb{R}^3$ with a connected complement and smooth orientable boundaries Γ_0 and Γ_1, respectively, such that $\overline{D}_1 \subset D_0$. Define $D := D_0 \setminus \overline{D}_1$ with boundary $\Gamma = \Gamma_0 \cup \Gamma_1$ and unit normal vector ν on Γ directed into the complement of D. Now Bernoulli's free boundary value problem consists in determining the exterior boundary Γ_0 such that the overdetermined boundary value problem

$$\Delta u = 0 \quad \text{in } D, \tag{1.1}$$

$$u = 0, \quad -\frac{\partial u}{\partial \nu} = \lambda \quad \text{on } \Gamma_0, \tag{1.2}$$

$$u = 1 \quad \text{on } \Gamma_1, \tag{1.3}$$

has a solution $u \in H^1(D)$. Here we assume the interior boundary Γ_1 to be known and λ to be a given positive constant. This Bernoulli problem has been studied for over more than fifty years and it is well understood mathematically. In three spatial dimensions the existence of the solution was established by Alt and Caffarelli [2] with the aid of variational methods and by Caffarelli and Spruck [3] and Acker [4] via the method of sub- and super-solutions for convex domains. Moreover, if the given interior boundary Γ_1 is convex then the free boundary Γ_0 is convex as well [5] and is unique [6].

* Corresponding author.
E-mail addresses: olhaivanyshyn@iyte.edu.tr (O.I. Yaman), kress@math.uni-goettingen.de (R. Kress).

http://dx.doi.org/10.1016/j.camwa.2017.06.011
0898-1221/

For the numerical solution of the Bernoulli free boundary problem in two dimensions various methods have been suggested among which we can distinguish two main groups: trial methods and methods based on shape optimization. A trial method is a fixed point iteration for the unknown free boundary: Given an initial guess for the free boundary Γ_0, firstly the boundary value problem (1.1)–(1.3) is solved with only one of the two boundary conditions at the free boundary and then secondly the other boundary condition is used for updating the free boundary. These two steps are iterated until both boundary conditions on Γ_0 are satisfied up to some specified accuracy, see [1,7–9]. The second strategy for the numerical solution of Bernoulli's problem is reformulating it as a shape optimization problem, see [10–13]. In three dimensions trial methods for the Bernoulli problem were investigated by Bugeanu and Harbrecht [14] and shape optimization methods by Harbrecht [15] and Ben Abda et al. [16].

Recently, motivated by ideas of Trefftz [17], a new method was suggested by one of us [18] for the numerical solution of the two dimensional Bernoulli problem. The method is based on a pair of boundary integral equations, which are linear with respect to the unknown flux over the interior boundary and nonlinear with respect to the free boundary. This system is solved by Newton iterations which converge locally with second order. The aim of this paper is to extend this approach to three dimensions.

The plan of the paper is as follows. In Section 2 we derive the system of nonlinear boundary integral equations and introduce their parametrization. Next, in our main Section 3 we elaborate Fréchet derivatives of boundary integral operators in a form that is well suited for the further theoretical and numerical study. In Section 4, the numerical implementation of the method is described and its feasibility is illustrated by numerical examples.

2. Nonlinear integral equations and parametrization

According to Green's formula the solution to the Bernoulli problem can be represented by

$$u(x) = \int_\Gamma \left\{ \frac{\partial u}{\partial \nu}(y)\Phi(x,y) - u(y)\,\frac{\partial \Phi(x,y)}{\partial \nu(y)} \right\} ds(y), \quad x \in D,$$

where

$$\Phi(x,y) = \frac{1}{4\pi}\frac{1}{|x-y|}, \quad x \neq y,$$

is the fundamental solution of the Laplace equation in three dimensions. By the jump relations for the single-layer potential and the boundary conditions (1.2)–(1.3) we obtain a system of boundary integral equations

$$-\lambda \int_{\Gamma_0} \Phi(x,y)\,ds(y) + \int_{\Gamma_1} \Phi(x,y) g(y)\,ds(y) = 0, \quad x \in \Gamma_0, \tag{2.1}$$

$$-\lambda \int_{\Gamma_0} \Phi(x,y)\,ds(y) + \int_{\Gamma_1} \Phi(x,y) g(y)\,ds(y) = 1, \quad x \in \Gamma_1, \tag{2.2}$$

for the unknowns Γ_0 and $g = \frac{\partial u}{\partial \nu}\big|_{\Gamma_1}$ which can be shown to be equivalent to the Bernoulli problem (1.1)–(1.3). The proof is analogous to that in [18, Theorem 2.1].

Introducing the single-layer potential operators $\mathcal{S}_{jk} : H^{-1/2}(\Gamma_k) \to H^{1/2}(\Gamma_j)$ defined by

$$(\mathcal{S}_{jk}\upsilon)(x) = \int_{\Gamma_k} \Phi(x,y)\upsilon(y)\,ds(y), \quad x \in \Gamma_j,$$

we rewrite the system (2.1)–(2.2) in a short operator form

$$-\lambda \mathcal{S}_{00} 1 + \mathcal{S}_{01} g = 0, \tag{2.3}$$

$$-\lambda \mathcal{S}_{10} 1 + \mathcal{S}_{11} g = 1. \tag{2.4}$$

The system is nonlinear with respect to the unknown free boundary Γ_0 and linear with respect to the unknown g. Furthermore, since the single-layer operator $\mathcal{S}_{11}$ is bijective, [19, Theorems 7.39 and 7.40], we can use Eq. (2.4) for finding the initial function g for the first step of our algorithm.

In order to linearize the boundary integral equations (2.3)–(2.4) and to solve them numerically we introduce a parametrization for the boundary surfaces, i.e., we assume that the surfaces Γ_0 and Γ_1 are C^2-smooth and homeomorphic to the unit sphere $\mathbb{S}^2$,

$$\Gamma_k := \{z_k(\widehat{x}) : \widehat{x} \in \mathbb{S}^2\}, \quad k = 0, 1,$$

and that Γ_0 has a star-shaped representation

$$z_0(\widehat{x}) = r(\widehat{x})\widehat{x}, \quad r(\widehat{x}) > 0,\ \widehat{x} \in \mathbb{S}^2.$$

Now the parametrized single-layer operators $S_{jk} : H^{-1/2}(\mathbb{S}^2) \to H^{1/2}(\mathbb{S}^2)$ such that $(\mathcal{S}_{jk}\upsilon) \circ z_j = S_{jk}(\upsilon \circ z_k)$ assume the form

$$(S_{jk}\widetilde{\upsilon})(\widehat{x}) = \int_{\mathbb{S}^2} \Phi(z_j(\widehat{x}), z_k(\widehat{y}))\widetilde{\upsilon}(\widehat{y}) J_{z_k}(\widehat{y})\,ds(\widehat{y}), \quad \widehat{x} \in \mathbb{S}^2, \tag{2.5}$$

where $\widetilde{\upsilon} = \upsilon \circ z_k$ and J_{z_k} is the Jacobian of the transformation. In the case of a star-shaped surface we have a simple expression of the Jacobian given by

$$J_r = r\sqrt{r^2 + |\mathrm{Grad}\, r|^2}, \tag{2.6}$$

where Grad denotes the surface gradient on $\mathbb{S}^2$. The parametrized form of the system (2.3)–(2.4) now reads

$$F\begin{pmatrix} r \\ \widetilde{g} \end{pmatrix} = \begin{pmatrix} 0 \\ 1 \end{pmatrix}, \tag{2.7}$$

where the nonlinear operator $F : C_+^2(\mathbb{S}^2) \times H^{-1/2}(\mathbb{S}^2) \to H^{1/2}(\mathbb{S}^2) \times H^{1/2}(\mathbb{S}^2)$ is defined by

$$F\begin{pmatrix} r \\ \widetilde{g} \end{pmatrix} := \begin{pmatrix} -\lambda S_{00}[1, r] + S_{01}[\widetilde{g}, r] \\ -\lambda S_{10}[1, r] + S_{11}\widetilde{g} \end{pmatrix}.$$

It is known, that the operator F is Fréchet differentiable [19]. In the next section we derive a form of the Fréchet derivative F' which is properly suited both for the theoretical investigation and the numerical implementation.

3. Fréchet derivatives of the parametrized operators

To investigate the derivatives we introduce spherical coordinates on $\mathbb{S}^2$ and define the unit vector in radial direction

$$\widehat{e}(\theta, \varphi) := (\sin\theta\cos\varphi, \sin\theta\sin\varphi, \cos\theta), \quad \theta \in [0, \pi], \ \varphi \in [0, 2\pi]. \tag{3.1}$$

The parametrized exterior unit normal ν to Γ_0 is given by

$$\nu \circ z_0 = \frac{r\widehat{e} - \mathrm{Grad}\, r}{\sqrt{r^2 + |\mathrm{Grad}\, r|^2}}, \tag{3.2}$$

where $\mathrm{Grad}\, r = r_\varphi/\sin^2\theta\, \widehat{e}_\varphi + r_\theta\, \widehat{e}_\theta$. For convenience we set $\widetilde{\nu} = \nu \circ z_0$.

Additionally, we introduce the double-layer potential operators by

$$(K_{jk}\widetilde{\upsilon})(\widehat{x}) = \frac{1}{4\pi}\int_{\mathbb{S}^2} \frac{[z_j(\widehat{x}) - z_k(\widehat{y})]\cdot\widetilde{\nu}(\widehat{y})}{|z_j(\widehat{x}) - z_k(\widehat{y})|^3}\,\widetilde{\upsilon}(\widehat{y}) J_{z_k}(\widehat{y})\, ds(\widehat{y}), \quad \widehat{x} \in \mathbb{S}^2, \tag{3.3}$$

and the derivative of the single-layer potential operator in the direction $\widehat{e}$ by

$$(L_{jk}\widetilde{\upsilon})(\widehat{x}) = \frac{-1}{4\pi}\int_{\mathbb{S}^2} \frac{[z_j(\widehat{x}) - z_k(\widehat{y})]\cdot\widehat{x}}{|z_j(\widehat{x}) - z_k(\widehat{y})|^3}\,\widetilde{\upsilon}(\widehat{y}) J_{z_k}(\widehat{y})\, ds(\widehat{y}), \quad \widehat{x} \in \mathbb{S}^2. \tag{3.4}$$

Theorem 3.1. *The Fréchet derivative of the operators S_{00}, S_{10} and S_{01} with respect to the shape function r can be represented in the form*

$$dS_{00}[1, r; q] = K_{00}\left(\frac{rq}{\sqrt{r^2 + |\mathrm{Grad}\, r|^2}}\right) + qL_{00}1 + S_{00}\left(\frac{2\widetilde{H}rq}{\sqrt{r^2 + |\mathrm{Grad}\, r|^2}}\right)$$

and

$$dS_{10}[1, r; q] = K_{10}\left(\frac{rq}{\sqrt{r^2 + |\mathrm{Grad}\, r|^2}}\right) + S_{10}\left(\frac{2\widetilde{H}rq}{\sqrt{r^2 + |\mathrm{Grad}\, r|^2}}\right)$$

and

$$dS_{01}[\widetilde{g}, r; q] = qL_{01}\widetilde{g},$$

where $\widetilde{H} = H \circ z_0$ in terms of the mean curvature H of the surface Γ_0.

Proof. The Fréchet derivative on the integral operators is obtained by differentiating their kernels with respect to z_0, see [19, Section 18.3] or [20]. Therefore

$$(dS_{00}[1, r; q])(\widehat{x}) = \frac{-1}{4\pi}\int_{\mathbb{S}^2} \frac{[z_0(\widehat{x}) - z_0(\widehat{y})]\cdot[q(\widehat{x})\widehat{x} - q(\widehat{y})\widehat{y}]}{|z_0(\widehat{x}) - z_0(\widehat{y})|^3} J_r(\widehat{y})\, ds(\widehat{y}) + \frac{1}{4\pi}\int_{\mathbb{S}^2} \frac{1}{|z_0(\widehat{x}) - z_0(\widehat{y})|} J_r' q(\widehat{y})\, ds(\widehat{y}), \tag{3.5}$$

where

$$J_r' q = q\sqrt{r^2 + |\mathrm{Grad}\, r|^2} + r\,\frac{rq + \mathrm{Grad}\, r \cdot \mathrm{Grad}\, q}{\sqrt{r^2 + |\mathrm{Grad}\, r|^2}}.$$

Elementary computations show that we can represent the unit vector $\widehat{e}$ in terms of normal and tangential components by

$$\widehat{e} = (\widehat{e}\cdot\widetilde{\nu})\widetilde{\nu} + \frac{1}{r^2+|\mathrm{Grad}\, r|^2}\left[r_\theta\frac{\partial z_0}{\partial\theta} + \frac{r_\varphi}{\sin^2\theta}\frac{\partial z_0}{\partial\varphi}\right].$$

In view of (3.2), this implies

$$\frac{1}{4\pi}\,\frac{z_0(\widehat{x})-z_0(\widehat{y})}{|z_0(\widehat{x})-z_0(\widehat{y})|^3}\cdot\widehat{y} = \frac{\partial\Phi(\widehat{x},\widehat{y})}{\partial\widetilde{\nu}(\widehat{y})}\,\frac{r(\widehat{y})}{\sqrt{r^2(\widehat{y})+|\mathrm{Grad}\, r(\widehat{y})|^2}} + \frac{\mathrm{Grad}_{\widehat{y}}\Phi(\widehat{x},\widehat{y})\cdot\mathrm{Grad}\, r(\widehat{y})}{r^2(\widehat{y})+|\mathrm{Grad}\, r(\widehat{y})|^2}.$$

Inserting this in (3.5), with the aid the Gauss surface divergence theorem we obtain that

$$dS_{00}[1,r;q] = qL_{00}1 + K_{00}\left(\frac{rq}{\sqrt{r^2+|\mathrm{Grad}\, r|^2}}\right) + S_{00}\psi,$$

where

$$\psi = -\frac{1}{r\sqrt{r^2+|\mathrm{Grad}\, r|^2}}\mathrm{Div}\frac{rq\,\mathrm{Grad}\, r}{\sqrt{r^2+|\mathrm{Grad}\, r|^2}} + \frac{q}{r} + \frac{rq+\mathrm{Grad}\, r\cdot\mathrm{Grad}\, q}{r^2+|\mathrm{Grad}\, r|^2}$$

and Div denotes the surface divergence on $\mathbb{S}^2$. The expression for ψ can be simplified to

$$\psi = \frac{q}{\sqrt{r^2+|\mathrm{Grad}\, r|^2}}\left[\frac{2r}{\sqrt{r^2+|\mathrm{Grad}\, r|^2}} - \mathrm{Div}\frac{\mathrm{Grad}\, r}{\sqrt{r^2+|\mathrm{Grad}\, r|^2}}\right].$$

Using (3.2) we can write

$$\frac{\mathrm{Grad}\, r}{\sqrt{r^2+|\mathrm{Grad}\, r|^2}} = -(\widetilde{\nu}\cdot\widehat{e}_\theta)\widehat{e}_\theta - \frac{1}{\sin\theta}\,(\widetilde{\nu}\cdot\widehat{e}_\varphi)\widehat{e}_\varphi.$$

From this, taking the surface divergence with the aid of the Weingarten formulas from differential geometry for the derivatives of $\widetilde{\nu}$ we obtain that

$$\mathrm{Div}\frac{\mathrm{Grad}\, r}{\sqrt{r^2+|\mathrm{Grad}\, r|^2}} = \frac{2r}{\sqrt{r^2+|\mathrm{Grad}\, r|^2}} - 2r\widetilde{H}$$

and consequently

$$\psi = \frac{q}{\sqrt{r^2+|\mathrm{Grad}\, r|^2}}\,2r\widetilde{H},$$

where in the definition of the curvature H we take the interior normal in order to guarantee that the curvature of the sphere is positive. This completes the proof for the operator S_{00}. The proofs for the operators S_{10} and S_{01} are analogous, see also [18] for the two-dimensional case. □

Writing down explicitly the Fréchet derivative of the operator F

$$F'_{r,\widetilde{g}}\begin{pmatrix}q\\ \widetilde{h}\end{pmatrix} = \begin{pmatrix}-\lambda\big(K_{00}(\mu_r\, q) + qL_{00}1 + S_{00}(2\widetilde{H}\mu_r\, q)\big) + qL_{01}\widetilde{g} + S_{01}\widetilde{h}\\ -\lambda\big(K_{10}(\mu_r\, q) + S_{10}(2\widetilde{H}\mu_r\, q)\big) + S_{11}\widetilde{h}\end{pmatrix}$$

with $\mu_r = r/\sqrt{r^2+|\mathrm{Grad}\, r|^2}$, we now can formulate the iterative scheme for the solution of the nonlinear system (2.7).

The iterative scheme.

Step 1. Choose an initial boundary parametrization with a radial function r and solve the parametrized form of the well-posed integral equation of the first kind (2.4) for the initial flux $\widetilde{g}$ over Γ_1.

Step 2. Given the approximation $(r,\widetilde{g})$ we solve the linearized system

$$F'_{r,\widetilde{g}}\begin{pmatrix}q\\ \widetilde{h}\end{pmatrix} = \begin{pmatrix}0\\ 1\end{pmatrix} - F\begin{pmatrix}r\\ \widetilde{g}\end{pmatrix}, \tag{3.6}$$

for q and $\widetilde{h}$.

Step 3. Update $r = r+q$ for the radial function and $\widetilde{g} = \widetilde{g}+\widetilde{h}$ for the boundary values.

Step 4. Repeat the last two steps until a stopping criterion is fulfilled.

For this iteration scheme we have the following local convergence theorem as main theoretical result.

Theorem 3.2. *Let $z_0 = r\widehat{e}$ be the parametrization of a convex free boundary Γ_0, z_1 be the parametrization of the interior boundary Γ_1 and let $\widetilde{g} = \big(\partial_\nu u|_{\Gamma_1}\big)\circ z_1$, where u is the solution to (1.1)–(1.3). Then there exists a neighborhood Ω of $(r,\widetilde{g})^T$ such that the Newton iterations (3.6) converge quadratically for each initial guess from Ω.*

Proof. Since the convex surface has a positive mean curvature we can follow the proof of [18, Theorem 3.1] and conclude that the Fréchet derivative $F'_{r,\widetilde{g}} : C^2_+(\mathbb{S}^2)\times H^{-1/2}(\mathbb{S}^2) \to C^2(\mathbb{S}^2)\times H^{1/2}(\mathbb{S}^2)$ is injective. Additionally, since due to Vogel [21] the free surface is analytic we can extend [18, Theorem 3.2] to three dimensions and obtain that $F'_{r,\widetilde{g}}$ is a homeomorphism at the exact solution. The Lipschitz condition is also fulfilled due to the fact that the operator $F'_{r,\widetilde{g}}$ is two times Fréchet differentiable. □

4. Numerical implementation and experiments

To solve the parametrized system of linear integral equations (3.6) we use the fully discrete Galerkin method by Ganesh and Graham [22] which is based on approximations by spherical harmonics and converges super algebraically in the case of smooth boundaries. The idea of the method was first suggested by Atkinson [23] and further developed by Wienert [24], see also [25, Subsection 3.6].

The kernels of the integral operators $S_{01}, S_{10}, K_{10}, L_{01}$ are smooth and therefore for their numerical approximation we can apply the Gauss trapezoidal product rule for numerical quadrature over the unit sphere

$$\int_{\mathbb{S}^2} f\,ds \approx Q_n(f) := \frac{\pi}{n+1}\sum_{\rho=0}^{2n+1}\sum_{\tau=1}^{n+1}\alpha_\tau f(\widehat{x}_{\tau,\rho}) \tag{4.1}$$

with the quadrature points

$$\widehat{x}_{\tau,\rho} = \widehat{e}\left(\arccos\theta_\tau, \frac{\rho\pi}{n+1}\right)$$

given in terms of the zeros ζ_τ of the Legendre polynomial P_{n+1} of degree $n+1$ and the Gauss–Legendre weights α_τ. The quadrature (4.1) is used in the definition of the projection operator

$$P_n f := \sum_{m=0}^{n}\sum_{\ell=-m}^{m} Q_n(f\overline{Y_n^\ell})Y_n^\ell \tag{4.2}$$

with an orthonormal basis of spherical harmonics Y_m^ℓ for $\ell = -m, \ldots, m$ and $m = 0, \ldots, n$. To approximate the operators with weakly singular kernels K_{00}, S_{00}, S_{11}, by an orthogonal transformation we move the singularity to the north pole $\widehat{n} = (0, 0, 1)^T$ and use a modified Gauss trapezoidal rule for the approximation of the weakly singular integral

$$\int_{\mathbb{S}^2}\frac{f(\widehat{x})}{|\widehat{n}-\widehat{x}|}\,ds(\widehat{x}) \approx \int_{\mathbb{S}^2}\frac{(P_n f)(\widehat{x})}{|\widehat{n}-\widehat{x}|}\,ds(\widehat{x}) = \frac{\pi}{n+1}\sum_{\rho=0}^{2n+1}\sum_{\tau=1}^{n+1}\beta_\tau f(\widehat{x}_{\tau,\rho}) \tag{4.3}$$

where

$$\beta_\tau = \frac{\pi\alpha_\tau}{n+1}\sum_{l=0}^{n} P_l(\zeta_\tau), \quad \tau = 1, \ldots, n+1.$$

This quadrature rule exploits the fact that the spherical harmonics are eigenfunctions of the single-layer potential operator on $\mathbb{S}^2$. For further details we refer to [22].

We also can apply this approximation for the discretization of $L_{00}1$ with the use of the transformation

$$(L_{00}1)(\widehat{x}) = -2\widehat{x}\cdot(S_{00}\widetilde{H}\widetilde{\nu})(\widehat{x}) - \widehat{x}\cdot(K_{00}\widetilde{\nu})(\widehat{x}), \quad \widehat{x}\in\mathbb{S}^2.$$

This follows from

$$\operatorname{Grad}\int_{\Gamma_0}\Phi(x,y)\,ds(y) = -2\int_{\Gamma_0}\Phi(x,y)\,ds(y) - \int_{\Gamma_0}\nu(y)\frac{\Phi(x,y)}{\partial\nu(y)}\,ds(y)$$

which is a consequence of the integral theorem

$$\int_{\Gamma_0}\operatorname{Grad}\varphi\,ds = 2\int_{\Gamma_0}H\varphi\,ds.$$

(see [26, Theorem 2.1]) and $\operatorname{Grad}_x\Phi(x,y) = -\operatorname{Grad}_y\Phi(x,y)$.

We note that the system (3.6) can be also solved by Wienert's variant of the spectral method as described in [24,25] and there is one-to-one correspondence between the solutions received by the two methods (see [27]).

We also need the explicit form of the mean curvature of a surface given by its radial function r. Lengthy computations yield

$$\begin{aligned}2r\sqrt{r^2+|\operatorname{Grad} r|^2}^{\,3}\,H\circ z_0 = {}& -(r^2+r_\theta^2)\,\Delta_S r + \left(r_\theta^2 - \frac{1}{\sin^2\theta}r_\varphi^2\right)r_{\theta\theta}\\ &+ \frac{2r_\varphi r_\theta}{\sin^2\theta}\left(r_{\theta\varphi} - r_\varphi\cot\theta\right) + r(2r^2+3|\operatorname{Grad} r|^2)\end{aligned} \tag{4.4}$$

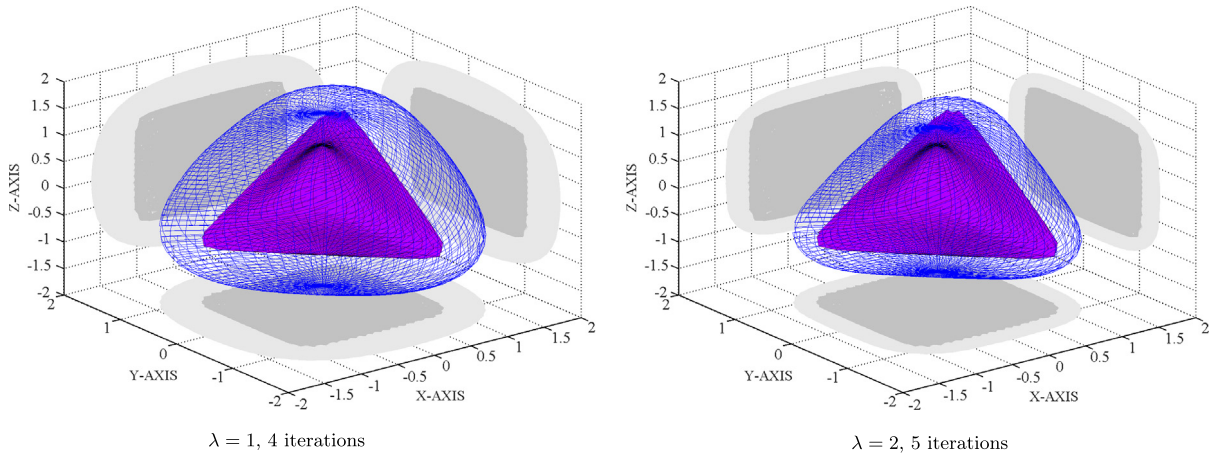

Fig. 1. Free boundary for Bernoulli's problem with convex interior domain.

where Δ_S denotes the Laplace–Beltrami operator on $\mathbb{S}^2$, that is,

$$\Delta_S r = r_{\theta\theta} + \frac{1}{\sin^2\theta} r_{\varphi\varphi} + r_\theta \cot\theta.$$

When r is a spherical harmonic (4.4) can be evaluated by using the recurrence relations for the associated Legendre polynomials occurring in the traditional basis of spherical harmonics and the fact that the latter are eigenfunctions of the Laplace–Beltrami operator.

To illustrate the feasibility of the method we present several numerical examples which include convex and non-convex interior domains and multiple interior domains of different types.

In the approximations of the integral operators in the system (3.6) we chose the following discretization parameters: the unknown radial function of the free boundary is approximated by a linear combination of real valued spherical harmonics of degree less than or equal to 8, the unknown flux on the boundary of each interior object is approximated by a linear combination of real valued spherical harmonics of degree less than or equal to 7. For the fully discrete version of the system (3.6) we used parameters $n = 12$ and $n = 7$ in the quadrature rules (4.1) and (4.3) for the integral operators evaluated over the free boundary Γ_0 and the boundary of each interior domain, respectively. The final discrete overdetermined system of linear equations is of size $(13^2 + 8^2 d) \times (9^2 + 8^2 d)$ where d is the number of interior domains and is solved via least squares for the unknown update $(q, \widetilde{h})^T \in H^{2.7}(\mathbb{S}^2) \times H^{-1/2}(\mathbb{S}^2)$, that is, with a Sobolev penalty term. For the first two examples with a single interior domain we chose as initial guess for Γ_0 a sphere of radius $R_0 = 2$ and for the examples with more than one interior component we increased the radius to $R_0 = 4$. The corresponding initial density $\widetilde{g}$ was found by solving the boundary integral equation (2.4). The iterations are stopped once the norm of the update in (3.6) is less than 10^{-5}.

In the first example we consider as interior domain D_1 a convex tetrahedral domain with the boundary parametrization described in [28]. As can be seen from Fig. 1, the free boundary is found very fast, in 5 iterations, and the behavior of the free boundary when λ increases corresponds to the expected one.

For the next example we chose a non-convex bean-like surface with the parametrization

$$z_0(\theta, \phi) = \begin{pmatrix} 1.6\sqrt{(1 - 0.1\cos(\pi\cos\theta))}\,\sin\theta\cos\varphi \\ 1.6\sqrt{(1 - 0.4\cos(\pi\cos\theta))}\,\sin\theta\sin\varphi - 0.6\cos(\pi\cos\theta) \\ 2\cos\theta \end{pmatrix}.$$

Although we proved convergence only for convex domains, the numerical experiments show that the method also works in the case of non-convex domains, Fig. 2.

The second group of examples is dedicated to interior objects D_1 with multiple components such that each of them has a connected complement. The behavior of the free boundary shown in Fig. 3 is similar to the one in [14].

The final examples present the solution when the interior domain consists of components of different types. In this case the free boundary was found in less than 10 iterations, Fig. 4.

Summarizing, the nonlinear integral equation method is well-suited for solving Bernoulli's free boundary value problem. The exploitation of the form of the Fréchet derivative that we derived facilitated the implementation since it gave us the chance to reapply the discretization of standard potential theoretic operators.

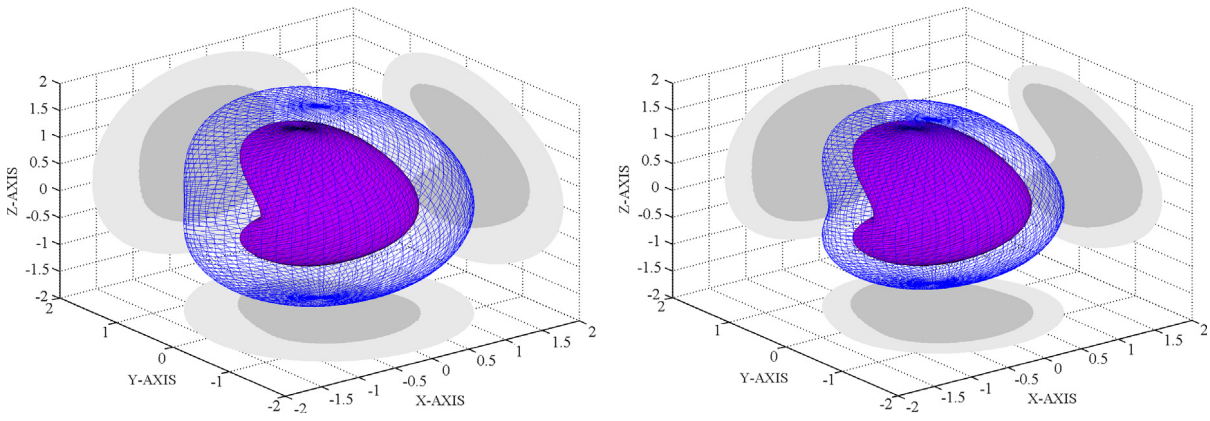

$\lambda = 1$, 4 iterations $\lambda = 2$, 4 iterations

Fig. 2. Free boundary for Bernoulli's problem with non-convex interior domain.

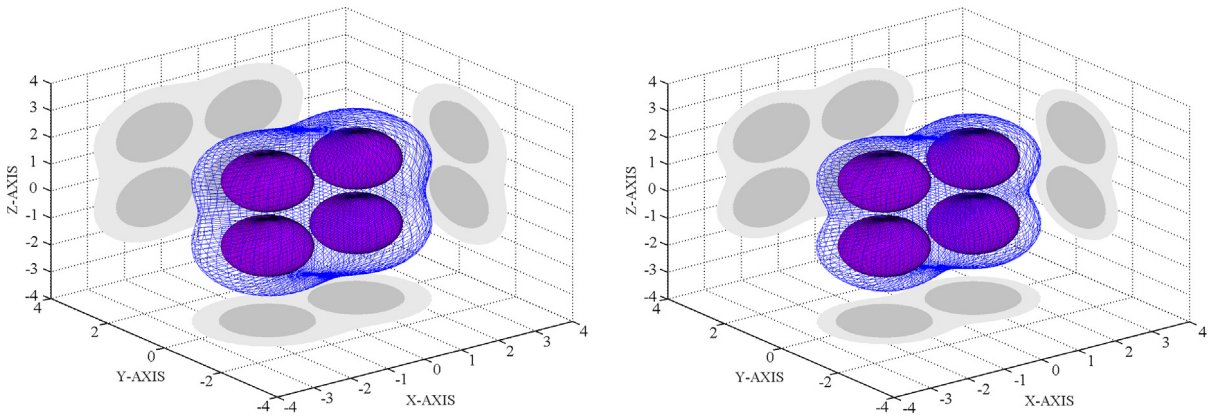

$\lambda = 1$, 5 iterations $\lambda = 1.5$, 5 iterations

Fig. 3. Free boundary for Bernoulli's problem with multi-component domain.

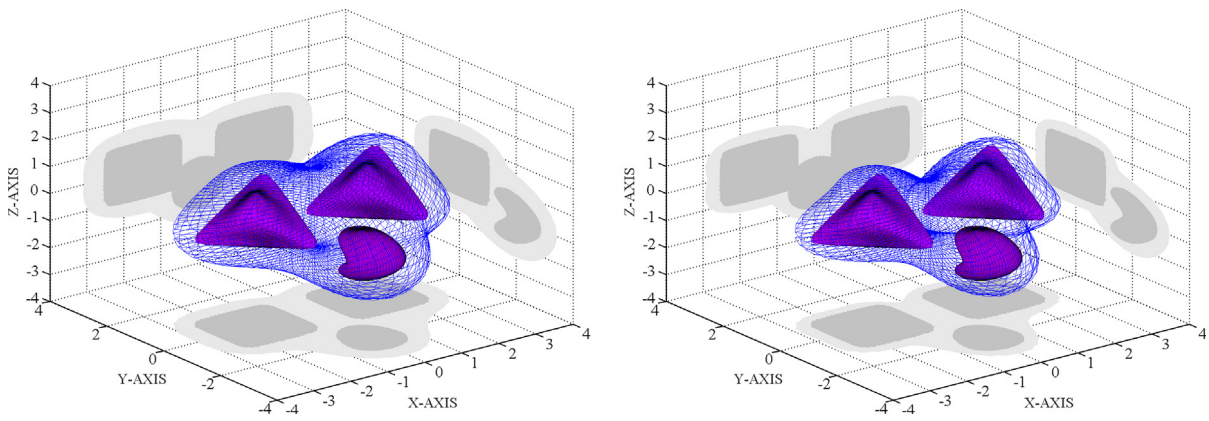

$\lambda = 1$, 6 iterations $\lambda = 1.5$, 9 iterations

Fig. 4. Free boundary for Bernoulli's problem with multi-component domain.

Acknowledgment

This research was initiated when O.I.Y. was visiting the GRK 2088 "Discovering Structure in Complex Data" at the University of Göttingen. The hospitality and the support are gratefully acknowledged.

References

[1] M. Flucher, M. Rumpf, Bernoulli's free-boundary problem, qualitative theory and numerical approximation, J. Reine Angew. Math. 486 (1997) 165–204.
[2] H.W. Alt, L.A. Caffarelli, Existence and regularity for a minimum problem with free boundary, J. Reine Angew. Math. 325 (1981) 105–144.
[3] L.A. Caffarelli, J. Spruck, Convexity properties of solutions to some classical variational problems, Comm. Partial Differential Equations 7 (11) (1982) 1337–1379.
[4] A. Acker, Uniqueness and monotonicity of solutions for the interior Bernoulli free boundary problem in the convex, *n*-dimensional case, Nonlinear Anal. 13 (12) (1989) 1409–1425.
[5] D.E. Tepper, A free boundary problem in an annulus, J. Aust. Math. Soc. Ser. A 34 (2) (1983) 177–181.
[6] A. Henrot, H. Shahgholian, Convexity of free boundaries with Bernoulli type boundary condition, Nonlinear Anal. 28 (5) (1997) 815–823.
[7] A. Acker, How to approximate the solutions of certain free boundary problems for the Laplace equation by using the contraction principle, Z. Angew. Math. Phys. 32 (1) (1981) 22–33.
[8] H. Harbrecht, G. Mitrou, Improved trial methods for a class of generalized Bernoulli problems, J. Math. Anal. Appl. 420 (1) (2014) 177–194.
[9] T. Tiihonen, J. Järvinen, On fixed point (trial) methods for free boundary problems, in: Free Boundary Problems in Continuum Mechanics, (Novosibirsk, 1991), in: Internat. Ser. Numer. Math., vol. 106, Birkhäuser, Basel, 1992, pp. 339–350.
[10] M.C. Delfour, J.-P. Zolésio, Shapes and Geometries, in: Advances in Design and Control, vol. 4, Society for Industrial and Applied Mathematics (SIAM), Philadelphia, PA, 2001, p. xviii+482 Analysis, differential calculus, and optimization.
[11] K. Eppler, H. Harbrecht, Shape optimization for free boundary problems—analysis and numerics, in: Constrained Optimization and Optimal Control for Partial Differential Equations, in: Internat. Ser. Numer. Math., vol. 160, Birkhäuser/Springer Basel AG, Basel, 2012, pp. 277–288.
[12] J. Haslinger, T. Kozubek, K. Kunisch, G. Peichl, Shape optimization and fictitious domain approach for solving free boundary problems of Bernoulli type, Comput. Optim. Appl. 26 (3) (2003) 231–251.
[13] K. Ito, K. Kunisch, G.H. Peichl, Variational approach to shape derivatives for a class of Bernoulli problems, J. Math. Anal. Appl. 314 (1) (2006) 126–149.
[14] M. Bugeanu, H. Harbrecht, A second order convergent trial method for a free boundary problem in three dimensions, Interfaces Free Bound. 17 (4) (2015) 517–537.
[15] H. Harbrecht, A Newton method for Bernoulli's free boundary problem in three dimensions, Computing 82 (1) (2008) 11–30.
[16] A. Ben Abda, F. Bouchon, G.H. Peichl, M. Sayeh, R. Touzani, A Dirichlet-Neumann cost functional approach for the Bernoulli problem, J. Engrg. Math. 81 (2013) 157–176.
[17] E. Trefftz, Über die Kontraktion kreisförmiger Flüssigkeitsstrahlen., Z. Math. Phys. 64 (1916) 34–61.
[18] R. Kress, On Trefftz' integral equation for the Bernoulli free boundary value problem, Numer. Math. 136 (2) (2017) 503–522.
[19] R. Kress, Linear Integral Equations, third ed., in: Applied Mathematical Sciences, vol. 82, Springer, New York, 2014, p. xvi+412.
[20] R. Potthast, Domain derivatives in electromagnetic scattering, Math. Methods Appl. Sci. 19 (15) (1996) 1157–1175.
[21] A.L. Vogel, Symmetry and regularity for general regions having a solution to certain overdetermined boundary value problems, Atti Semin. Mat. Fis. Univ. Modena 40 (2) (1992) 443–484.
[22] M. Ganesh, I.G. Graham, A high-order algorithm for obstacle scattering in three dimensions, J. Comput. Phys. 198 (1) (2004) 211–242.
[23] K.E. Atkinson, The numerical solution of Laplace's equation in three dimensions. I., SIAM J. Numer. Anal. 19 (1982) 263–274.
[24] L. Wienert, Die numerische Approximation von Randintegraloperatoren für die Helmholtzgleichung im $\mathbb{R}^3$, Univ. Göttingen, Math.-Naturwiss. Fachber., Göttingen, 1990, p. 92s.
[25] D. Colton, R. Kress, Inverse Acoustic and Electromagnetic Scattering Theory, third ed., in: Applied Mathematical Sciences, vol. 93, Springer, New York, 2013, p. xiv+405.
[26] D. Colton, R. Kress, Integral Equation Methods in Scattering Theory, in: Classics in Applied Mathematics, vol. 72, Society for Industrial and Applied Mathematics (SIAM), Philadelphia, PA, 2013, p. xvi+271.
[27] I.G. Graham, I.H. Sloan, Fully discrete spectral boundary integral methods for Helmholtz problems on smooth closed surfaces in $\mathbb{R}^3$, Numer. Math. 92 (2) (2002) 289–323.
[28] S. Onaka, Simple equations giving shapes of various convex polyhedra: The regular polydedra and polyhedra composed of crystallographically low-index planes, Phil. Mag. Lett. 86 (3) (2006) 175–183.